International Journal of Electrical, Electronic and Communication Sciences
ISSN: 2517-9438
Vol:10, No:6, 2016

Parametrization of Piezoelectric Vibration Energy Harvesters for Low Power Embedded Systems

Yannick Verbelen, Tim Dekegel, Ann Peeters, Klara Stinders, Niek Blondeel, Sam De Winne, An Braeken, Abdellah Touhafi

Abstract—Matching an embedded electronic application with a cantilever vibration energy harvester remains a difficult endeavour due to the large number of factors influencing the output power. In the presented work, complementary balanced energy harvester parametrization is used as a methodology for simplification of harvester integration in electronic applications. This is achieved by a dual approach consisting of an adaptation of the general parametrization methodology in conjunction with a straight forward harvester benchmarking strategy. For this purpose, the design and implementation of a suitable user friendly cantilever energy harvester benchmarking platform is discussed. Its effectiveness is demonstrated by applying the methodology to a commercially available Mide V21BL vibration energy harvester, with excitation amplitude and frequency as variables.

Keywords—Energy harvesting, vibrations, piezoelectric transducers, embedded systems, harvester parametrization.

I. Introduction

THE introduction of microcontroller technology with a stand-by power consumption in the μW range and a deep sleep power consumption below 1 μW has led to a broad range of novel embedded electronic applications with an ever increasing life span [38, p. 628], [22]. Bluetooth Low Energy (BLE, Bluetooth 4.0) beacons are an emerging technology in this power consumption range [14]. In Internet-Of-Things (IoT), the CC2540/CC2564 SoCs for BLE [32] continue to push Zigbee [24] out of the consumer as well as industrial market [28], [10], [19], [16] while ESP8266 series system-on-chip (SoC) devices with integrated wireless connectivity are superseding dedicated transceiver modules on the WiFi side of the spectrum [3], [46], [31]. In the lowest power range, it is currently possible to design embedded electronic applications with an estimated battery life exceeding the projected life time of the application itself, therefore eliminating any periodic battery replacement from the perspective of the user [34]. However, the tight power requirements limit application functionality, making a performant user interface difficult, and commercial battery performance leaves much to be desired. Users would not realize the devices contain batteries because they never had to be replaced, resulting in an elevated risk of these devices being disposed in landfills instead of being collected as hazardous waste to recover the precious materials batteries contain. To eliminate the environmental concerns related to the use of batteries in mass-produced devices [43] and improve their functionality for the user, an alternative power source is necessary that can either complement the battery [44] or replace it completely. Energy harvesters as auxiliary power sources have considerable potential because they convert energy from the application's environment to electrical power, have a life span up to dozens of years, and may function both as power generator and as sensor [1], [7], [33]. These properties make them a favoured choice in the power supply design of various autonomous wireless sensing applications where a very long life time is desired [12], [39].

Yannick Verbelen is with the Vrije Universiteit Brussel, Pleinlaan 2, 1050 Etterbeek, Brussels, Belgium (Corresponding author; e-mail: yannick.verbelen@vub.ac.be).

While energy harvester technology has received increasing interest in recent years and is under continuous development, only three harvester types are sufficiently mature and have a power output that is large enough to be of use in practical electronic applications: photovoltaics, thermoelectrics and piezoelectrics [43], [4]. Despite the large normal power output (in mW/cm^2) of photovoltaic cells, their usefulness is limited to applications that are exposed to natural or artificial light sources [25, table I, p. 262]. This is rarely the case in industrial environments such as manufacturing facilities, steel mills, raw material processing, power generation etc., where wireless sensing applications are commonly required to remotely monitor the operation of said facilities. Kinetic energy is fortunately abundantly available in any industrial environment, usually in the form of vibrations propagating through rigid structures such as buildings and machines mechanically coupled to moving parts of motors, generators, pumps, etc. [35], [17], [6], and even on human resources operating these facilities [49], [15]. These vibrations are an otherwise unused source of power, hence converting them to electric power is a true energy scavenging application [44]. The same vibrations can simultaneously be used to monitor operation of the vibrating equipment, doubling as a sensor, thus further increasing the usefulness of vibration energy harvesters in wireless sensing applications.

A major difficulty with vibration energy harvesters is that the power output is a function of multiple parameters, making vibration energy harvesting a multidimensional problem [11]. The amplitude of the vibrations, their frequency spectrum, the shape of the harvester, its orientation and even the strategy used to mechanically connect it to the vibration source, all influence the harvester's power output [50]. This complexity limits their ease of use, and power supply designers will often prefer easier to use power sources, such as batteries or photovoltaics, over vibration harvesters even when an abundant vibration source is available. In an effort to solve this problem, a simple yet powerful methodology to parametrize vibration harvesters is necessary. To this purpose, we apply a novel methodology for parametrization of energy harvesters

[45].

II. Existing Implementations

Numerous implementations of test setups for vibration energy harvesters have been discussed in literature. In [48], Yang et al. describe a shaker based implementation for testing electrodynamic vibration energy harvesters with planar coils [48, Fig. 6, p. 5]. An accelerometer is used as feedback. A similar approach is suggested by Challa et al. using a function generator and amplifier to create a variable vibration source [8, Fig. 7, p. 6]. Unfortunately, automated frequency sweeps are not possible with such a setup. Korla et al. apply partial automation, and focus on low frequency vibrations for a compact harvester using a very large shaker as vibration source [23, Fig. 3, p. 267]. Leland et al. [26] and Ertruk et al. [13] use a vibrometer in conjunction with an accelerometer for contactless vibration measurements. To measure generated power, Liu et al. propose two strategies: Direct dissipation in a load resistor and indirect power measurement through the Joule effect (1), and AC measurement through a full bridge rectifier [27, Fig. 5, p. 804](2). Other sources confirm this approach [23], although optimizations are possible by using Schottky or tunnel diodes instead of silicon diodes [23, Fig. 2a, p. 267]. Since a shaker offers the most flexible frequency and amplitude range [40], this is the approach of choice for the implementation described in this article.

III. Harvester Parametrization Methodology

The energy harvester parametrization methodology discussed in [45] presents the output power of any generic energy harvester as the product of three factors μ_g, p_g and η_g:

$$P_g(t) = \mu_g \cdot p_g(\mu_g) \cdot \eta_g(t) \tag{1}$$

P_g is the power output of any given harvester g, μ_g is its size in ς (with $\varsigma = 1\,\mathrm{cm}^2$ for vibration harvesters), p_g its normalized power output with $[p_g] = \frac{W}{\varsigma}$, and η_g the harvester's efficiency. For vibration harvesters, different parameters can now be attributed to one of the 3 factors in the equation above. The parameter p_g expresses the normalized maximum power output of a harvester, i.e. independent of the harvester's size. Due to the large discrepancy between properties of electromagnetic and piezoelectric harvesters, this work exclusively focuses on cantilever based piezoelectric harvesters, as bistable vibration harvesters are covered by He et al. in recent literature [18]. For cantilever piezoelectric harvesters, p_g corresponds to the normalized power rating when a sinusoidal excitation at the harvester's resonance frequency is applied that leads to the maximal tip displacement [30]. As material properties of p_g, both the resonance frequency and maximal tip displacement are harvester properties that can be found in harvester datasheets.

Unlike other harvesters, such as photovoltaic cells, the power output of vibration harvesters at maximum excitation and tip displacement ($\eta_g \approx 1$) is not only a function of the material properties of p_g and the size of the harvester μ_g, but also strongly depends on the geometry of the harvester. This geometry is in turn a determining factor for the harvester's resonance frequency. Fig. 1 shows a comparison of the normalized output power p_g at an excitation of 1 g for various vibration energy harvesters in their respective resonance frequencies. Since all harvesters are composed of identical piezoelectric material operated at identical excitation in their respective resonance frequencies, the differences in p_g are solely attributed to the differences in harvester geometry. Resonance frequencies are also shown to illustrate that the differences cannot be traced to the disparity in harvestable energy at different frequencies. While a somewhat accurate mathematical correlation between harvesters of similar geometry can be deducted, the methodology is excessively complicated because harvester geometry is a subjective parameter that makes adequate comparison between harvesters from different series or manufacturers difficult. The energy harvester parametrization methodology described in [45] is fortunately flexible enough to be adapted to these specific constraints. When η_g is retained as a metric for the offset between the ideal excitation amplitude/frequency combination and the actual operating conditions, the parameters p_g and μ_g can be combined to represent the harvester's specific maximum power output, taking into account the harvester's material composition, geometry and size. This simplification is in fact an extension of the methodology in [45] as a special case where $\varsigma \neq 1\,\mathrm{cm}^2$, but instead ς equals the size of the harvester itself. Equation (1) remains valid and can be used transparently in the parametrization methodology. The dependence on a specific $\varsigma \neq 1\,\mathrm{cm}^2$ can be expressed as

$$P_g(t) = [\mu_g]_\varsigma \, [p_g]_\varsigma \, \eta_g(t) \qquad [\mu_g]_\varsigma \in \mathbb{N}^+ \tag{2}$$

where $[p_g]_\varsigma$ represents the normalized maximum power output of a single harvester of a specific type, model, geometry etc., and $[\mu_g]_\varsigma$ is the total harvester area expressed as a number of harvesters of that specific type, model and geometry. Therefore $[\mu_g]_\varsigma$ is a positive natural number unlike in (1) where $\mu_g \in \mathbb{R}^+$. The conclusion that μ_g is a constant multiple of the intrinsic harvester size is a result of the demonstrated effect of harvester geometry which cannot be transparently quantized and must subsequently be excluded from the equation to allow further modelling.

Variables related to η_g are parameters that can be varied: Most notably excitation amplitude, frequency range,

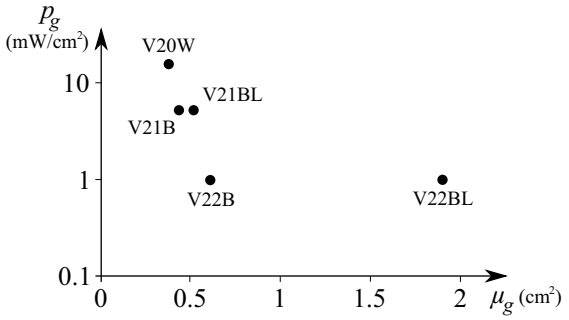

Fig. 1 Comparison of the power outputs of various Mide vibration energy harvesters under a load of 1 g at their respective resonance frequencies

mechanical adhesion and harvester orientation. A testing environment must be able to vary these variables to mimic real environmental conditions in which the harvester might be used.

IV. Testbed Design

A test bed for piezoelectric cantilever vibration energy harvesters must be capable of modulating the variables affecting η_g, most notably the amplitude of the vibration measured in g (with $1\,\mathrm{g} \approx 9.81\,\mathrm{m/s^2}$) and the frequency of the vibration measured in Hz. To eliminate anomalies caused by variations in mechanical adhesion and orientation, harvesters must be mounted in a known standardized position. This section discusses the design considerations and implementation of a low cost test bed for piezoelectric cantilever vibration energy harvesters, and how this can be integrated in the harvester parametrization methodology presented above. The proposed design consists of a closed loop vibration generator using a commercial shaker as vibration source and an accelerometer as the necessary sensor providing frequency and amplitude feedback. The harvester is then mounted on the vibration generator with a variable impedance as load to measure its power and maximum power point, and enable simulation of impedance matching with loads such as buffer capacitors or DC/DC converters. Fig. 2 shows a block diagram of the test setup.

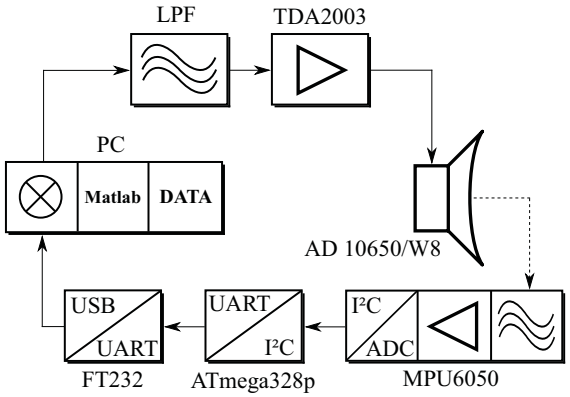

Fig. 2 Block diagram of the benchmarking platform with an AD 10650/W8 subwoofer as vibration source, TDA2003 as amplifier and MPU6050 as vibration sensor

A. Vibration Generator

Three potential vibration generators were compared: A DC motor with asymmetric load as commonly used in game controllers and mobile phones, a piezoelectric material with a voltage applied to it, and finally a traditional speaker. Experiments quickly ruled out the first two options. Both DC motors and piezoelectric crystals are not suitable as generators for this application because the amplitude with which they vibrate is either too variable or too small, respectively. Speakers in heavy duty implementation ("shaker"), commonly used as subwoofers in the audio industry, are considerably better suited since both the amplitude and the frequency are easily controllable. This design choice is consistent with literature describing shakers in similar applications as vibration sources [42, Fig. 9a, p. 4], [8], [13].

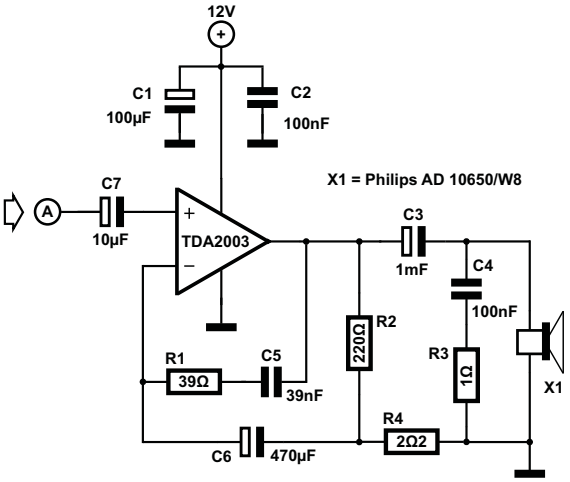

Fig. 3 Schematic diagram of the TDA2003 based amplifier circuit driving the subwoofer [41]

A type AD 10650/W8 from Philips with a diameter of 10 inches and nominal impedance of 8 Ω was selected as shaker based on its favourable impedance [20] and wide frequency response. A standard TDA2003 10 W audio amplifier was connected to drive it with sinusoidal excitation signals [41]. This amplifier has a bandwidth of nearly 15 kHz (40 Hz to 15 kHz at -3 dB attenuation for an output power of 1 W in a load of 4 Ω) and a maximum gain of 40 dB, while keeping distortion low at typically 0.15 % at 1 kHz. These properties greatly simplify the amplifier design because the TDA2003's frequency response in conjunction with the shaker's natural attenuation of higher frequencies eliminates the need of extensive input and output filtering to remove harmonics. Fig. 3 shows the schematic diagram of the amplifier design.

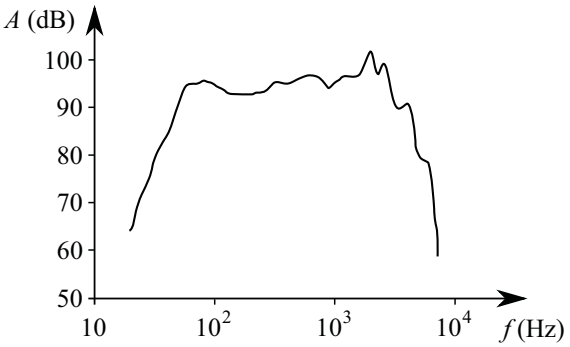

Fig. 4 Frequency response of the Philips AD 10650/W8 subwoofer [20]

A recurring issue with commercial shakers is the irregular frequency response that is insufficiently flat to qualify as excitation source for vibration harvester benchmarking. One possible solution to this problem is measuring the frequency response, as shown in Fig. 4 and then compensating it in

software by means of a look up table (LUT) in which the inverse frequency response is stored. While this works adequately for a short period of time, mechanical wear and decay of the shaker's membranes cause a continuous slow drift of the frequency response which in turn leads to a constantly increasing error decreasing the compensation's effectiveness. Since it is a cumbersome task to measure or model this wear over time and adjust the LUT accordingly, it was chosen to use a closed loop feedback instead of open loop amplitude regulation. For this purpose an accelerometer was selected as low cost vibration sensor. A platform was manufactured in ABS plastic using additive 3D printing technology to accommodate accelerometers and piezoelectric DUTs, and was attached to the conus of the shaker using epoxy glue.

B. Accelerometer Selection Criteria

The accelerometer must be selected with care, as accelerometer performance is paramount to a vibration with stable amplitude and frequency. The responsiveness is of particular importance for the frequency sweeps used in automated testing, as discussed below. Modern MEMS accelerometers are very low cost due to their widespread use in mobile gadgets such as mobile phones, game controllers and drones, and nearly all except the cheapest ones have specifications that generously exceed the requirements for this test bed. Accelerometers with a range up to 16 g are readily available, often with selectable sensitivity. To eliminate noise contamination of analog output signals, a MEMS accelerometer with integrated ADC is advised. As of 2016, MEMS accelerometers with an I^2C interface are becoming the norm, surpassing older devices with three analog output channels. The MPU6050 from InvenSense has dynamically reprogrammable sensitivity ranging from ± 2 g up to ± 16 g [9]. At 16 bits resolution, the highest sensitivity corresponds to 16384 LSB/g which exceeds the sensitivity of commercial sensors for comparable purposes such as the LOG-0002-025G-PC from Mide (0.0008 g resolution at 16 bit ADC) for only a fraction of the cost [37], [21].

While low cost MEMS accelerometers have adequate resolution, sensitivity, and sample frequency (up to 1 kHz for MPU6050) a recurringly cited drawback is the noise on measurements reducing actual resolution of 16 bit devices to 14 bits or less. The low cost of these devices allows them to be combined into arrays, however, creating kinematically redundant sensor systems. Output can be processed by averaging values from different devices to eliminate random noise, or advanced accelerometer array algorithms can be implemented [2], [29]. A diagram of the test bench setup is shown in Fig. 5.

C. Software

A pc has been chosen as data processing unit to reduce the cost of external hardware and to take advantage of Matlab as DSP platform and user control interface. Data from the accelerometer is sampled at 512 Hz and transmitted to the pc, using an FT232 UART to USB bridge well documented in literature [36]. A standard ATmega328p microcontroller

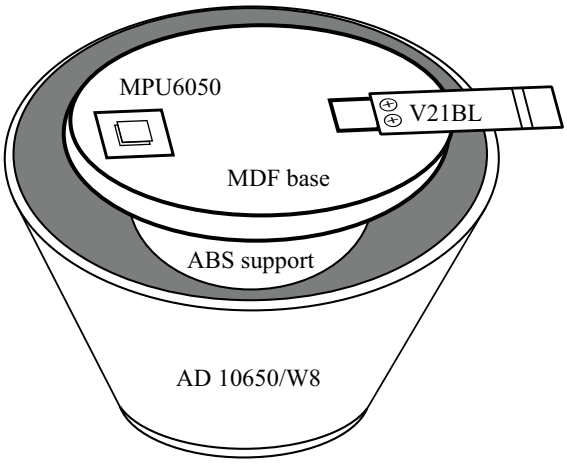

Fig. 5 Test bench setup with subwoofer and accelerometer.

was chosen to configure the accelerometer using its I^2C interface and to read out its data. Accelerometer samples are transmitted to the pc and processed in Matlab with a Fast Fourier Transformation (FFT) to extract amplitude and frequency information from a series of 512 samples (1 s data) at a time. Choosing a multiple of 2 ($512 = 2^9$) speeds up the FFT computation which benefits the response time of the control loop. Fig. 2 shows the different hardware blocks and their respective connection protocols. An example output of the FFT operation in Matlab is shown in Fig. 6 for a 25 Hz sinusoidal signal with an amplitude of 0.35 g.

V. Design Verification

The properties of the implemented test bench must be checked and verified prior to the measurement of actual energy harvesters. It is particularly important to quantize the errors on amplitude and frequency of the asserted signal, and ensure that second order effects such as harmonics, noise and distortion are within the acceptable accuracy margins. This can be achieved by verifying the shaker's frequency response, whose irregularity is compensated in software by means of a proportional regulator. The output amplitude of the sinusoidal control signal for the shaker will automatically be adjusted to compensate for its attenuation of low and high frequencies, ideally resulting in a constant vibration amplitude regardless of the frequency. This is an essential requirement for testing since both amplitude and frequency are independent factors that influence η_g and thus must be treated as variables in the equation. An automated calibration and test routine was implemented in Matlab to generate a frequency sweep from 1 Hz up to 500 Hz with an accuracy of 1 Hz. Below a frequency of 15 Hz it was discovered that the attenuation of the shaker prohibits a satisfactory linear amplitude selection in the range from 0 to ± 3 g with a minimum accuracy of 0.01 g. However, a cut-off frequency of 15 Hz is acceptable because all commercially available cantilever piezoelectric vibration energy harvesters are designed to operate at frequencies higher than 15 Hz. An example analysis at a frequency of 25 Hz is

shown in Fig. 6, with the accelerometer data in both time and frequency domain.

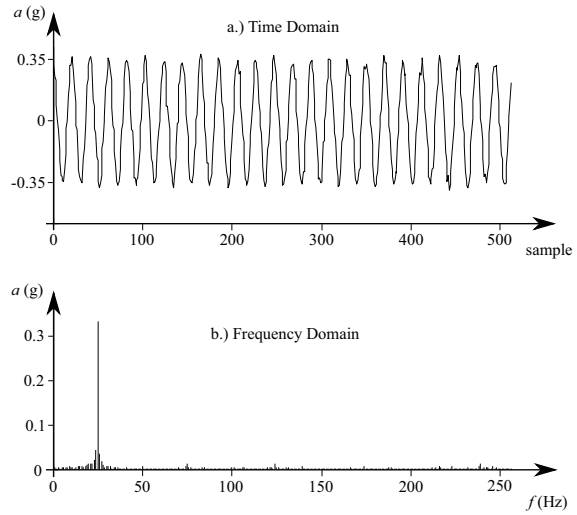

Fig. 6 Frequency response of the subwoofer as accelerometer samples in time domain (a) and in frequency domain (b)

The error on the amplitude is less than 1 % over the entire frequency spectrum between 15 Hz and 200 Hz in a range ±3 g. Minor spectral leakage can be seen in Fig. 6 around the center frequency of 25 Hz as a result of aliasing caused by the 512 sample input for the FFT. Fig. 7 demonstrates the frequency response from the perspective of the shaker. A near linear correlation exists between peak to peak input voltage (Vpp) and vibration amplitude for all frequencies in the 25 Hz - 200 Hz range, but the response for center frequencies (most notably 125 Hz - 150 Hz) is over three times stronger than limit frequencies for the same input Vpp. Measurements were verified with a second accelerometer of type MMA7361.

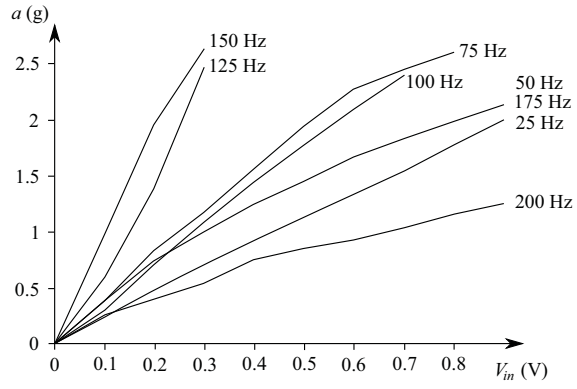

Fig. 7 Frequency response of the subwoofer as function of the input voltage for different frequencies

VI. Harvester Parametrization

A. Amplitude - Frequency Sweep Analysis

With the intended operation of the test bed verified, actual cantilever piezoelectric vibration energy harvesters can be tested under varying vibration amplitude and frequency to determine their power output. A Matlab algorithm was developed that sweeps frequency and amplitude over independently configurable ranges with a step of choice. The function takes 6 arguments: The lowest frequency, frequency step, highest frequency, lowest amplitude, amplitude step and highest amplitude. The generated power is then rectified and buffered with a capacitor to allow the measurement of average power instead of peak power, and finally dissipated in a digitally controlled potentiometer of type MCP4151. With a maximum voltage of 5.5 V, resistance of 100 kΩ and a resolution of 8 bits, the load can be adjusted with increments of approx. 390 Ω which is sufficiently accurate to represent the load of a real world DC/DC converter [47], [5]. Using the load impedance, the measured output voltage is converted in a power rating using Ohm's Law since the load is a purely resistive impedance. Fig. 8 shows the result of a frequency and amplitude sweep for a V21BL vibration energy harvester from Mide, captured in its maximum power point (MPP) as shown in Fig. 9. Note that unlike vibration amplitude or frequency the operation point on the load line cannot be considered a true variable of η_g since the power path will often contain a form of MPPT to ensure operation in the MPP on the load line. For real world harvester applications, the power point may for this reason be excluded from η_g, simplifying (2). The relatively constant load impedance presented to the harvester by a DC/DC converter will make a continuous load impedance sweep largely obsolete. The MCP4151 can subsequently be replaced with a constant load resistor to operate the harvester in its maximum power point without inducing errors in the power output measurements.

B. Modelling the Power Output

Matlab generates threedimensional diagrams as a graphical representation of the amplitude and frequency sweep data for a specified load impedance. Every load impedance results in a separate graph.

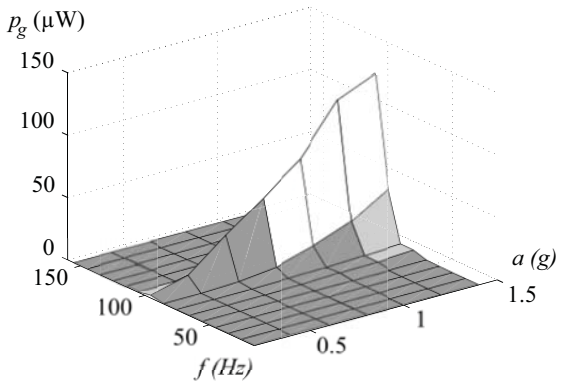

Fig. 8 Power output of a V21BL vibration harvester as a function of vibration amplitude and frequency

It is immediately apparent that the harvester only generates useful output power when operated at its resonance frequency

or very close to it. For any other frequencies, the harvester does not produce significant output power. Before modelling η_g as a function of amplitude a and frequency f, it is a prequirement to determine whether a correlation exists between a and f. Fortunately, the correlation between both variables is insignificant, determined by numerical correlation computation. It can also directly be deducted from Fig. 8 that both variables do not influence each other with statistical significance. This allows the effect of a and f to be modelled independently. For a constant load Z in the harvester's MPP, η_g can be expressed as

$$\eta_g\left(a, f, Z\right) = \frac{a}{a_0} \cdot \frac{f}{f_0} \tag{3}$$

with a_0 the excitation amplitude at which maximum output power occurs and f_0 the frequency at which maximum power point occurs.

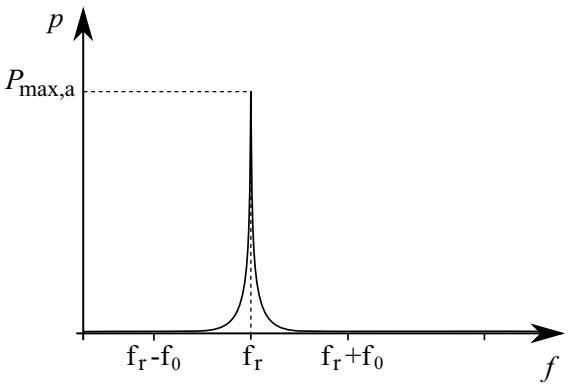

Fig. 9 Exponential approximation of the resonance frequency f_r with maximum power output $P_{max,a}$

At any given vibration a, the power output of the harvester resembles a narrow peak with steep slopes, shown in Fig. 9. Since this curve is a cross section of Fig. 8 across the y axis, the maximum of the curve occurs at the resonance frequency f_r with an amplitude equal to the maximum power output of the harvester at a vibration a, $P_{max,a}$. Using regression to prove curve symmetry and data point correlation, the slope approximates an exponential curve with negative exponent of the form e^{-bf} where b determines the steepness and shape (with $b > 0$), and f is the frequency variable. From the symmetry around the resonance frequency f_r the equation of the curve in Fig. 9 can be modelled as

$$P_{o,a,f} = P_{max,a} \cdot e^{-b|f-f_r|} \tag{4}$$

The parameter b must be obtained by calculating the equation of an exponential trend line on the slope of any cross section as seen in Fig. 9, based on experimental data points. Similarly a cross section along the x axis yields a curve representing the power output for a frequency f at any amplitude a. This curve can be approximated by a linear relation between the power output at that frequency $P_{max,f}$ and the excitation amplitude a. The equation of this curve follows directly from linear trigonometry:

$$P_{o,a,f} = P_{max,f} \frac{a}{a_{max}} \tag{5}$$

Expressions (4) and (5) can now be combined to obtain a model for η_g since

$$\frac{a}{a_0} = \frac{P_{o,a,f}}{P_{max,a}} = e^{-b|f-f_r|} \tag{6}$$

and

$$\frac{f}{f_0} = \frac{P_{o,f,a}}{P_{max,f}} = \frac{a}{a_{max}} \tag{7}$$

due to a and f being uncorrelated variables. Combining these equations with (3) results in an expression for $\eta_g(a, f)$ and in turn a power output for the harvester in the model for harvester parametrization presented in [45]:

$$P_g\left(t, a, f\right) = \left[\mu_g\right]_\varsigma \left[p_g\right]_\varsigma \frac{a}{a_{max}} e^{-b|f-f_r|} \tag{8}$$

With all limiting factors described in datasheets or deductible from statistical analysis of benchmarking data, this equation serves as a harvester specific expression of output power as a function of vibration amplitude and frequency.

VII. Future Work

The current implementation has considerable potential for complementary balanced energy harvesting applications by streamlining the design and development process through simplification of the harvester's characterization procedure. However, it still has several limitations: The cut-off frequency of 15 Hz prevents harnessing the energy of slower vibration sources such as movement from animals, including humans. A focus for further research will be the expansion of the testing environment to enable characterization of harvesters at smaller vibration frequencies, enabling testing of electromagnetic harvesters as well. The current amplitude range would also be insufficient for this purpose and also requires an upgrade. This upgrade will also allow destructive testing, allowing the estimation of the harvester's life time in its intended application rather than extrapolating the manufacturer's theoretical values.

Secondly, in this research it was assumed that conventional power path electronics provide an operation point close to the maximum power point of the harvester by means of adaptive MPP tracking. Although these electronics may be a favourable design choice to maximize power transfer and minimize harvester size accordingly, it is possible to design a system topology where the rectified harvester output is directly powering a system if it can cope with variations in voltage on its power rail. In this situation it is suspected that the impact of this impedance offset may no longer have a negligible effect on η_g and must be modelled as a third variable in (3).

Finally, the current experimental setup does not allow to measure the energy transfer efficiency from the test bed's surface to the harvester. This was mitigated by normalizing the attachment of the harvester to the test bed following the manufacturer's guidelines. This ensures that the same harvester in a field application would show the same performance, assuming it has been attached to the vibration source following these same guidelines. A contactless method should be developed to measure the energy transfer function of the mechanical energy into the harvester, without changing the harvester's resonance frequency or damping coefficient.

VIII. Conclusion

This paper applied the general methodology for the parametrization of energy harvesters for complementary balanced embedded systems to the specific case of cantilever piezoelectric vibration energy harvesters. Commercially available vibration harvesters demonstrated that the geometry of vibration harvesters is a decisive factor for their power output, preventing a distinction between p_g and μ_g. A solution for this problem was presented, considering a harvester with unity size ς instead of 1. This allowed the geometry and size of the harvester to be decoupled from its efficiency determined by vibration amplitude and vibration frequency. A test bed for automated harvester parametrization was designed and implemented, and measurements indicate no direct correlation between amplitude and frequency, allowing both variables to be modelled independently. The paper concluded with a derivation of a general expression for the power output of cantilever piezoelectric vibration energy harvesters, which was modelled as $P_g\left(t,a,f\right)=\left[\mu_g\right]_\varsigma\left[p_g\right]_\varsigma\frac{a}{a_{max}}e^{-b|f-f_r|}$.

Acknowledgement

The authors would like to thank the Flemish Agency for Innovation through Science and Technology (Agentschap voor Innovatie door Wetenschap en Technologie, IWT) for providing the funds that enabled this research in the context of the IPEH TETRA project. The 3D prints for the prototype were generously sponsored by and manufactured in Fablab Brussels.

References

[1] Ahmad, T. J., Arsalan, M., Black, M. J. et al., *Piezoelectric Based Flow Power Harvesting for Downhole Environment*, SPE Middle East Intelligent Oil and Gas Conference and Exhibition, Society of Petroleum Engineers, pp. 1-8, doi:10.2118/176777-MS, 2015.

[2] Amrs, S. W., Townsend, C. P., Churchill, D. L., et al., *Energy harvesting, wireless structural health monitoring system*, U.S. Patent No. 7,719,416, filed 11 September 2006, published 18 May 2010.

[3] Ashraf, Q. M., Yusoff, M. I. M., Azman, A. A. et al., *Energy monitoring prototype for Internet of Things: Preliminary results*, in 2015 IEEE 2nd World Forum on Internet of Things (WF-IoT), pp. 1-5, doi:10.1109/WF-IoT.2015.7389157, 2015.

[4] Bandyopadhyay, S. and Chandrakasan, A. P., *Platform Architecture for Solar, Thermal, and Vibration Energy Combining With MPPT and Single Inductor*, in IEEE J. Solid-State Circuits, vol. 47, no. 9, pp. 2199-2215, ISSN 0018-9200, doi:10.1109/JSSC.2012.2197239, 2012.

[5] Barbehenn, G. H., *True Grid Independence: Robust Energy Harvesting System for Wireless Sensors Uses Piezoelectric Energy Harvesting Power Supply and Li-Poly Batteries with Shunt Charger*, in J. Analog Innovation, vol. 20, no. 3, 2010.

[6] Berger, A., Hörmann, L. B., Leitner, C. et al., *Sustainable energy harvesting for robust wireless sensor networks in industrial applications*, in IEEE Sensors Applications Symposium (SAS) pp. 1-6, doi:10.1109/SAS.2015.7133585, 2015.

[7] Cahill, P., O'Keeffe, R., et al. *Structural Health Monitoring of Reinforced Concrete Beam Using Piezoelectric Energy Harvesting System*, 7th European Workshop on Structural Health Monitoring, pp. 189-196, hal-01020338, 2014.

[8] Challa, V. R., Prasad, M. G., Shi, Y. et al., *A vibration energy harvesting device with bidirectional resonance frequency tunability*, in Smart Materials and Structures, vol. 17, no. 1, pp. 1-10, doi:10.1088/0964-1726/17/01/015035, 2008.

[9] Chen, S., Wang, L., Jiang, et al., *A study on reliability of chip scale packages in shock environments*, in Proc. 14th Int. Conf. Electronic Packaging Technology (ICEPT), pp. 921-924, doi:10.1109/ICEPT.2013.6756611, 2013.

[10] Cho, K., Jung, C., Kim, J. et al., *Modelnig and analysis of performance based on Bluetooth Low Energy*, in 7th IEEE Latin-American Conf. Communications (LATINCOM), pp. 1-6, ISBN 978-1-4673-8450-6, doi:10.1109/LATINCOM.2015.7430115, 2015.

[11] Dekegel, T., *Ontwikkeling van een testbed voor piëzo-elektrische energy harvesters*, Master thesis, unpublished, Vrije Universiteit Brussel, Brussels, Belgium, 2015.

[12] Deng, L., Wen, Z., et al., *High Voltage Output MEMS Vibration Energy Harvester in Mode With PZT Thin Film*, in J. Microelectromechanical Systems, vol. 23, no. 4, pp. 855-861, ISSN 1057-7157, doi:10.1109/JMEMS.2013.2296034, 2014.

[13] Erturk, A., HOffmann, J., Inman, D. J., *A piezomagnetoelastic structure for broadband vibration energy harvesting*, in Applied Physics Letters, vol. 94, no. 25, doi:10.1063/1.3159815, 2009.

[14] Galinina, O., Mikhaylov, K., Andreev, S. et al., *Internet of Things, Smart Spaces, and Next Generation Networks and Systems: Wireless Sensor Network Based Smart Home System over BLE with Energy Harvesting Capability*, Springer, vol. 8638, pp. 419-432, doi:10.1007/978-3-319-10353-2_37, 2014.

[15] Green, P. L., Papatheou, E. and Sims, N. D., *Energy harvesting from human motion and bridge vibrations: An evaluation of current nonlinear energy harvesting solutions*, in J. Intelligent Material Systems and Structures, vol. 24, no. 12, pp. 1494-1505, doi:10.1177/1045389X12473379, 2013.

[16] Grover, M., Pardeshi, S. K., Singh, N., et al., *Bluetooth low energy for industrial automation*, in Proc. 2nd Int. Conf. Electronics and Communication Systems (ICECS), pp. 512-215, ISBN 978-1-4799-7224-1, doi:10.1109/ECS.2015.7124960, 2015.

[17] Hadas, Z., Vetiska, V., Huzlik, R. et al., *Model-based design and test of vibration energy harvester for aircraft application*, in Microsystem Technologies, vol. 20, no. 4, pp. 831-843, ISSN 0946-7076, doi:10.1007/s00542-013-2062-y, 2014.

[18] He, Q., Mao, X., Chu, D., *Output Performance Analysis on a Two-degrees-of-Freedom Bistable Piezoelectric Vibration Generator*, Int. J. Online Engineering, vol. 11, no. 6, 2015.

[19] Huang, Q. and Chen, K., *The Implementation of a Wireless Scale Based on Bluetooth 4.0 Low-energy*, in Proc. 2015 Int. Industrial Informatics and Computer Engineering Conf. (IIICEC), Atlantis Press, 2015.

[20] Hull, M. D., Eng., C., *Building Hi-Fi Speaker Systems*, Philips, 1980.

[21] Jaafar, I. S. S. A. and Czarnecki, Z., *Miniaturized low cost wireless data logger for vibration recording of physiological activities*, in IEEE Sensors, pp. 1-4, ISSN 1930-0395, doi:ICSENS.2013.6688256, 2013.

[22] Jones, M. H. and Scott, J. B., *The Energy Efficiency of 8-bit Low-power Microcontrollers*, in Proc. 18th Electronics New Zealand Conf. 2011.

[23] Korla, S., Leon, R. A., Tansei, I. N. et al., *Design and testing of an efficient and compact piezoelectric energy harvester*, in J. Microelectronics, vol. 42, no. 2, pp. 265-270, doi:10.1016/j.mejo.2010.10.018, 2011.

[24] Krishna, B. J. and Vadivukkarasi, K., *Energy Efficient Lightening System for an Indoor Environmnet using Wireless Sensor Network Based on IoT*, in Int. J. Research and Scientific Innovation (IJRSI), vol. 3, no. 5, pp. 144-148, ISSN 2321-2705, 2016.

[25] Kulah, H. and Najafi, K., *Energy Scavenging From Low-Frequency Vibrations by Using Frequency Up-Conversion for Wireless Sensor Applications*, in IEEE Sensors J., vol. 8, no. 3, pp. 261-268, ISSN 1530-437X, doi:10.1109/JSEN.2008.917125, 2008.

[26] Leland, E. S., and Wright, P. K., *Resonance tuning of piezoelectric vibration energy scavenging generators using compressive axial preload*, in Smart Materials and Structures, vol. 15, no. 5, pp. 1413-1420, doi:10.1088/0964-1726/15/5/030, 2006.

[27] Liu, J.-Q., Fang, H.-B., Xu, Z.-Y. et al., *A MEMS-based piezoelectric power generator array for vibration energy harvesting*, in J. Microelectronics, vol. 39, no. 5, pp. 802-806, doi:10.1016/j.mejo.2007.12.017, 2008.

[28] Mackensen, E., Lai, M., Wendt, T. M., *Bluetooth Low Energy (BLE) based wireless sensors*, in IEEE Sensors, pp. 1-4, ISSN 1930-0395, ISBN 978-1-4577-1766-6, doi:10.1109/ICSENS.2012.6411303, 2012.

[29] Madgwick, S. O. H., Harrison, A. J. L., Sharkey, P. M., et al., *Measuring motion with kinematically redundant accelerometer arrays: Theory, simulation and implementation*, in Mechatronics, vol. 23, no. 5, pp. 518-529, doi:10.1016/j.mechatronics.2013.04.003, 2013.

[30] Miso, K., Hoegen, M., Dugundji, J. et al., *Modeling and experimental verification of proof mass effects on vibration energy harvester performance*, in Smart Materials and Structures, vol. 19, no. 4, doi:10.1088/0964-1726/19/4/045023, 2010.

[31] Nadee, C., Chamnongthai, K., *Ultrasonic array sensors for monitoring of human fall detection*, in Proc. 12th Int. Conf. Electrical Engineering/Electronics, Computer, Telecommunications and Information Technology (ECTI-CON), pp. 1-4, doi:10.1109/ECTICon.2015.7207097 2015.
[32] Naik, A. G., Kuwelkar, S. and Magdum, V., *Evaluation of Classic Bluetooth Based On the Spectrums For Its Usability In Industrial Applications*, Int. J. Advanced Research in Electronics and Communication Engineering (IJARECE), vol. 4, no. 3, 2015.
[33] Parker, J. S., Roberts, S. *Vibration energy harvester for converting mechanical vibrational energy into electrical energy*, U.S. Patent No. 8,680,694, 2014.
[34] Penella, M., Albesa, J., Gasulla, M., *Powering wireless sensor nodes: primary batteries versus energy harvesting*, in Proc. IEEE Instrumentation and Measurement Technology Conf. (I2MTC), pp. 1625-1630, ISBN 978-1-42443353-7, 2009.
[35] Ren, L., Chen, R., Xia, H. et al., *Energy harvesting performance of a broadband electromagnetic vibration energy harvester for powering industrial wireless sensor networks*, in Proc. SPIE 9799, Active and Passive Smart Structures and Integrated Systems, 97993P, doi:10.1117/12.2218736, 2016.
[36] Sharma, M., Agarwal, N., Reddy, S. R. N., *Design and development of daughter board for USB-UART communication between Raspberry Pi and PC*, in Proc. Int. Conf. Computing, Communication & Automation (ICCCA), pp. 944-948, ISBN 978-1-4799-8889-1, 10.1109/CCAA.2015.7148532, 2015.
[37] Shieh, P. J., Azana, N. T., Santos, T. E. A., et al., *Methodology for choosing piezoelectric devices*, in Proc. IEEE Brasil RFID, pp. 46-49, ISBN 978-1-4799-7045-2, doi:10.1109/BrasilRFID.2014.7128963, 2014.
[38] Singh, K., Awasthi, A. K., *Quality, Reliability, Security and Robustness in Heterogenous Networks*, 9th Int. Conf. QShine 2013: Revised Selected Papers, 1011 p., Springer, 2013.
[39] Sodano, H. A., Inman, D. J., *Comparison of Piezoelectric Energy Harvesting Devices for Recharging Batteries*, in J. Intelligent Material Systems and Structures, vol. 16, no. 10, pp 799-807, doi:10.1177/1045389X05056681, Los Alamos National Laboratory, 2005.
[40] Sodano, H. A., Park, G. and Inman, D. J., *Estimation of Electric Charge Output for Piezoelectric Energy Harvesting*, in Strain, vol. 40, pp. 49-58, doi:10.1111/j.1475-1305.2004.00120.x, 2004.
[41] ST Microelectronics, *10 W Car Radio Audio Amplifier*, ST Microelectronics, datasheet, 2013.
[42] Tang, X., Lin, T., Zuo, L, *Design and optimization of a tubular linear electromagnetic vibration energy harvester*, IEEE Transactions on Mechatronics, vol. 19, no. 2, pp. 615-622, doi:10.1109/TMECH.2013.2249666, 2014.
[43] Verbelen, Y., Touhafi, A., *Resource Considerations for Durable Large Scale Renewable Energy Harvesting Applications*, in Proc. 2nd Int. Conf. Renewable Energy Research and Applications (ICRERA), pp. 401-406, doi:10.1109/ICRERA.2013.6749788, 2013.
[44] Verbelen, Y., Braeken, A., Touhafi, A., *Parametrization of Ambient Energy Harvesters for Complementary Balanced Electronic Applications*, in Proc. SPIE 8763, Smart Sensors, Actuators, and MEMS VI, 87631U, doi:10.1117/12.2018490, 2013.
[45] Verbelen, Y., Braeken, A., Touhafi, A., *Towards a complementary balanced energy harvesting solution for low power embedded systems*, in Microsystem Technologies, vol. 20, no. 4, pp. 1007-1021, doi:10.1007/s00542-014-2103-1, 2014.
[46] Volcko, T., Moucha, V., Kan, V., *A Wireless Communication Interfaces for Small Unmanned Systems*, in Proc. Int. Scientific Conf. Modern Safety Technologies in Transportation, pp. 200-205, ISSN 1338-5232, 2015.
[47] Whitaker, M., *Energy Harvester Produces Power from Local Environment, Eliminating Batteries in Wireless Sensors*, in J. Analog Innovation, vol. 20, no. 1, 2010.
[48] Yang, B., Lee, C., Xiang, W. et al., *Electromagnetic energy ahrvesting from vibrations of multiple frequencies*, in J. Micromechanics and Microengineering, vol. 19, no. 3, doi:10.1088/0960-1317/19/3/035001, 2009.
[49] Yang, W., Chen, J., Zhu, G. et al., *Harvesting Energy from the Natural Vibration of Human Walking*, in ACS Nano, vol. 7, no. 12, pp. 11317-11324, doi:10.1021/nn405175z, 2013.
[50] Zuo, L. and Tang, X., *Large-scale vibration energy harvesting*, in J. Intelligent Material Systems and Structures, vol. 24, no. 11, pp. 1405-1430, doi:10.1177/1045389X13486707, 2013.